**Supplemental Information of**

# Myelo- and cytoarchitectonic microstructural and functional human cortical atlases reconstructed in common MRI space

**Authors**
Rory Pijnenburg[1]*, Lianne H. Scholtens[1]*, Dirk Jan Ardesch[1], Siemon C. de Lange[1], Yongbin Wei[1], and Martijn P. van den Heuvel[1,2].

**Affiliations**
[1]Department of Complex Trait Genetics, Center for Neurogenomics and Cognitive Research, Faculty of Science, Vrije Universiteit Amsterdam, Amsterdam Neuroscience, Amsterdam, The Netherlands
[2]Department of Child Psychiatry, Amsterdam University Medical Center, Amsterdam Neuroscience, Amsterdam, The Netherlands

*equal contribution

**Corresponding author**
Lianne H. Scholtens, Vrije Universiteit Amsterdam, Amsterdam Neuroscience, Room: B-636, De Boelelaan 1081-1087, 1081 HV, Amsterdam, The Netherlands; Email: l.h.scholtens@vu.nl

## Supplemental Methods

### *Atlas consistency and segmentation number*

To evaluate the effect of building labels on 1 vs multiple subjects, we revisited the 20 subjects used for manual label segmentation in our previous project digitizing the Von Economo atlas (Scholtens et al. 2018). We implemented a sliding window approach, dividing the 20 manually segmented datasets into an atlas building set (N=15) and a test set (N=5) and constructed the .gcs atlas files based on 1, 2, 3, … up to 15 datasets. Then, for each of the 20 iterations in the sliding window approach, we applied each of the resulting 30 atlas versions (15 per hemisphere) to the 5 remaining subjects. For each atlas version, for each region label in the atlas, we calculated the vertex-wise overlap of the automatically generated labels with the manual segmentations, and averaged these scores to compute the average atlas segmentation consistency per hemisphere.

*Atlas generation - example code*

Example BASH code to generate an annotation (*.annot*) and subsequent atlas (*.gcs*) files from label (*.label*) files.

```
# initialization
DATA_DIR= # Directory including colortable file (.ctab)
LABEL_DIR= # Directory including individual label files (.label)
SUBJECT_DIR= # Directory including Freesurfer dataset

# generate annotation file from individual label files
mris_label2annot --ctab ${DATA_DIR}/lh.colortable.ctab --ldir
${LABEL_DIR} --annot annotationName --s colin27 --h lh --no-unknown
mris_label2annot --ctab ${DATA_DIR}/rh.colortable.ctab --ldir
${LABEL_DIR} --annot annotationName --s colin27 --h rh --no-unknown

# generate atlas file from annotation file
mris_ca_train lh lh.sphere.reg lh.annotationName.annot colin27
lh.atlasName.gcs
mris_ca_train rh rh.sphere.reg rh.annotationName.annot colin27
rh.atlasName.gcs
```

## Supplemental Results

### *Atlas consistency and segmentation number*

The average consistency for the set of 20 N=1 atlases was 0.7060 (std. 0.0268) for the left and 0.7172 (std. 0.0192) for the right hemisphere, with the average atlas performance improving to respectively 0.7820 (std. 0.0103) and 0.7897 (std. 0.007) for the N=15 atlases, very closely approximating the consistency reported for the full N=20 atlas presented in earlier work (Scholtens et al., 2018). These results (also depicted in Supplemental Figure S11), indicate that atlas performance indeed initially increases when incorporating more individual segmentations into the atlas construction, though the automatic-manual label consistency of the set of N=1 atlases still appears of a reasonably high level.

**Table S1. Region list Campbell atlas.** A list of all region names included in the original atlas and the digital atlas. Both the original and digital version of the 1905 Campbell atlas consist of 17 regions in total (Campbell 1905).

| Regions Original | Digital version |
|---|---|
| Prefrontal | prefrontal |
| Frontal | frontal |
| Precentral | precentral |
| Inter-precentral | inter_precentral |
| Postcentral | postcentral |
| Inter-postcentral | inter_postcentral |
| Parietal | parietal |
| Temporal | temporal |
| Visuo-sensory | visuosensory |
| Visuo-psychic | visuopsychic |
| Audio-sensory | audiosensory |
| Audio-psychic | audiopsychic |
| Olfactory | olfactory |
| Limbic A | limbicA |
| Limbic B | limbicB |
| Limbic C | limbicC |
| Insula | insula |

**Table S2. Region list Smith atlas.** A list of all region names included in the original atlas and the digital atlas. In total 43 regions are included in both the original and digital version of the 1907 Smith atlas (Smith 1907).

| Regions Original | Digital version |
|---|---|
| Callosal A | callosA |
| Callosal B | callosB |
| Callosal C | callosC |
| Callosal D | callosD |
| Frontal A | froA |
| Frontal B | froB |
| Frontal C | froC |
| Frontal D | froD |
| Frontal Inferior | froinf |
| Frontal Interior | froint |
| Frontal Interior B | frointB |
| Frontal Orbitofrontal | froorb |
| Frontal Superior | frosup |
| Frontal Superior-anterior | frosupant |
| Insula Inferior | insinf |

| | |
|---|---|
| Insula Postcentral | inspostc |
| Insula Precentral | insprec |
| Occipital Parastriatal | occparastr |
| Occipital Parietal | occpar |
| Occipital Peristriatal | occperistr |
| Occipital Striatal | occstr |
| Occipital Temporal | occtemp |
| Paradentate | paradent |
| Parasplenialis | paraspl |
| Paratemporal | temppara |
| Parietal Inferior A | parinfA |
| Parietal Inferior B | parinfB |
| Parietal Inferior C | parinfC |
| Parietal Superior A | parsupA |
| Parietal Superior B | parsupB |
| Parietal Olfactory | parolfact |
| Postcentral A | postcentA |
| Postcentral B | postcentB |
| Precentral A | precentA |
| Precentral B | precentB |
| Prefrontal | froprefro |
| Pyriform | pyriform |
| Temporal Heschl's gyri | tempheschl |
| Temporal Inferior | tempinf |
| Temporal Medial | tempmed |
| Temporal Pole | temppole |
| Temporal Superior | tempsup |
| Visuo-auditory band Alpha | vis-aud-bnd |
| Visuo-sensory band Beta | vis-sen-bnd |

**Table S3. Region list Brodmann atlas.** A list of all region names included in the original atlas and the corresponding regions in the digital atlas. The original 1909 Brodmann human atlas consists of 46 regions, the digital atlas contains 39 regions (Brodmann 1909).

| **Regions Original** | **Digital version** |
|---|---|
| BA1; BA3 | BA1_3 |
| BA2 | BA2 |
| BA4 | BA4 |
| BA5 | BA5 |
| BA6 | BA6 |
| BA7 | BA7 |
| BA8 | BA8 |

| | |
|---|---|
| BA9 | BA9 |
| BA10 | BA10 |
| BA11 | BA11 |
| BA13 | BA13 |
| BA16 | BA16 |
| BA17 | BA17 |
| BA18 | BA18 |
| BA19 | BA19 |
| BA20 | BA20 |
| BA21 | BA21 |
| BA22 | BA22 |
| BA23 | BA23 |
| BA24 | BA24 |
| BA25 | BA25 |
| BA26; BA29; BA30 | BA26_29_30 |
| BA27 | BA27 |
| BA28 | BA28 |
| BA31 | BA31 |
| BA32 | BA32 |
| BA33 | BA33 |
| BA34 | BA34 |
| BA35; BA36 | BA35_36 |
| BA37 | BA37 |
| BA38 | BA38 |
| BA39 | BA39 |
| BA40 | BA40 |
| BA41; BA42; BA52 | BA41_42_51 |
| BA43 | BA43 |
| BA44 | BA44 |
| BA45 | BA45 |
| BA46 | BA46 |
| BA47 | BA47 |

**Table S4. Region list Flechsig atlas.** A list of region names included in the original atlas and the corresponding regions in the digital atlas. The original 1920 Flechsig atlas consists of 53 regions and the digital atlas of 46 regions (both numbers include subdivisions of larger areas) (Flechsig 1920).

| **Regions Original** | **Digital version** |
|---|---|
| F2 | F2 |
| F2b | F2b |
| F3; F3b | F3 |

| | |
|---|---|
| F4; F4b; F4c | F4 |
| F5; F5a; 5' | F5 |
| F6 | F6 |
| F7 | F7 |
| F8 | F8 |
| F9 | F9 |
| F10 | F10 |
| F10x | F10x |
| F11 | F11 |
| F12 | F12 |
| F13 | F13 |
| F14; F14b | F14 |
| F15 | F15 |
| F16 | F16 |
| F17 | F17 |
| F18; F18a | F18 |
| F19 | F19 |
| F20 | F20 |
| F21 | F21 |
| F22 | F22 |
| F23 | F23 |
| F24 | F24 |
| F25 | F25 |
| F26 | F26 |
| F27 | F27 |
| F28 | F28 |
| F29 | F29 |
| F30 | F30 |
| F31 | F31 |
| F32 | F32 |
| F33 | F33 |
| F34 | F34 |
| F35 | F35 |
| F36 | F36 |
| F37 | F37 |
| F38 | F38 |
| F39 | F39 |
| F40 | F40 |
| F41 | F41 |
| F42 | F42 |

| | |
|---|---|
| F43 | F43 |
| F44 | F44 |
| F45 | F45 |

**Table S5. Region list Von Economo's cortical types atlas.** A list of all region descriptions included in the original- and the digital atlas. Von Economo's cortical type atlas contains 5 major cortical types and one intermediate type (von Economo and Koskinas 1925). We advise to merge labels within one cortical type for analyses.

| Regions Original | Digital version |
|---|---|
| Type 1 | CT1 |
| Type 1-2; inferior frontal | CT1_2_fro_inf |
| Type 1-2, medial orbitofrontal | CT1_2_mof |
| Type 1-2, precentral, insula, postcentral | CT1_2_prec_ins_postc |
| Type 1-2, temporal | CT1_2_temp |
| Type 2, frontal | CT2_fro |
| Type 2, parietal | CT2_par |
| Type 3, frontal | CT3_fro |
| Type 3, parietal | CT3_par |
| Type 4, occipital | CT4_occ |
| Type 4, dorsomedial prefrontal | CT4_dmpf |
| Type 5, central sulcus | CT5_cen |
| Type 5, insula | CT5_ins |
| Type 5, medial | CT5_med |
| Type 5, occipital | CT5_occ |

**Table S6. Functional specialization of brain regions as defined by Karl Kleist.** Overview of the regional functions as originally defined by Kleist (Kleist 1934). For each region the corresponding Brodmann area number was provided. Kleist's subdivisions were assigned an additional underscore and number as suffix (e.g. areas 40_1 and 40_2). Merged brain regions were marked with combined Brodmann area numbering linked by underscores (e.g. area 11_12). In addition, the description of the function of that region (translated from German into English) is provided.

| Region | Function (Translation from German to English) |
|---|---|
| 1_3a_3b | Touch sensation, Pain sensation, Temperature sensation |
| 2 | Kinesthetic sensation |
| 4 | Individual movements |
| 6aa | Dexterity, Power perception, Tone and sound formation |
| 6ab_1 | Trunk turning |

| | |
|---|---|
| 6ab_2 | Head turning |
| 7 | Action (sensory) leg, trunk |
| 8_1 | Falling and pointing reactions |
| 8_2 | Ocular turning |
| 9 | Initiative, Awareness of effort and power |
| 10 | Motor skill |
| 11_12 | Personal and social ego |
| 17_1 | Vision: brightness, colors, forms, movements |
| 17_2 | Visual field, lower quadrant |
| 17_3 | Visual field, upper quadrant |
| 18_1 | Sense of place, Eye movements, Optic awareness |
| 18_2 | Conjugate downward eye movements |
| 18_3 | Conjugate upward eye movements |
| 19_1 | Calculation, Recognition of numbers, Reading, Visual thinking, Visual recognition |
| 19_2 | Place memory |
| 19_3 | Color and object recognition |
| 20 | Appreciation of sounds and music |
| 21 | Hearing movements, Acoustic awareness |
| 22a_1 | Noise understanding |
| 22a_2 | Melody understanding |
| 22b_1 | Word understanding |
| 22b_2 | Sentence understanding |
| 23_24_26_29_30_31_32_33 | Corporeal ego (personal experience/awareness) |
| 28_34 | Olfactory recognition |
| 35_36 | Objective olfactory movements |
| 37 | Name understanding |
| 39_1 | Constructive action (sensory) |
| 39_40 | Body image, Right-Left orientation |
| 40_1 | Individual consecutive action |
| 40_2 | Recognition by touch |
| 40_3 | Face activity (sensory) |
| 41_42_52 | Sound/melody sensation, Noise sensation, Loudness sensation |
| 43 | Taste |
| 44a | Melody-, word formation |
| 44b | Name speaking (spontaneous) |
| 45 | Sentence speaking |
| 46 | Constructive thinking |
| 47 | Sentiment/Attitude, Mood-affected actions, Perseverance |

**Table S7. Asymmetric atlas pair consistency.** This table describes the global atlas-pair consistency, quantifying the extent to which cortical regions contained within a pair of atlases occupy the same area of cortex. For example, most Kleist regions are a subdivision of Brodmann's atlas, resulting in a large consistency between these atlases (see also Figure 4A).

| | **Brodmann** | **Campbell** | **EconomoCT** | **Flechsig** | **Kleist** | **Smith** |
|---|---|---|---|---|---|---|
| **Brodmann** | - | 0.75 | 0.74 | 0.60 | 0.89 | 0.58 |
| **Campbell** | 0.55 | - | 0.64 | 0.49 | 0.53 | 0.54 |
| **EconomoCT** | 0.55 | 0.67 | - | 0.54 | 0.49 | 0.53 |
| **Flechsig** | 0.64 | 0.77 | 0.75 | - | 0.63 | 0.64 |
| **Kleist** | 0.97 | 0.77 | 0.75 | 0.66 | - | 0.61 |
| **Smith** | 0.62 | 0.77 | 0.74 | 0.62 | 0.60 | - |

**Table S8. Digitized Brodmann region overlap with Fischl (2008) *ex vivo* labels.** This table lists for each *ex vivo* Brodmann area included in Fischl (2008) (BA?_exvivo_thresh) the matching digitized region label, the number of vertices on Colin27's surface (averaged across both hemispheres), the number of overlapping vertices, as well as the proportion of overlap.

| **label name** | | **N Vertices** | | | **proportion of overlap** | |
|---|---|---|---|---|---|---|
| ***ex vivo* Brodmann** | **digitized Brodman** | ***ex vivo*** | **digitized** | **overlap** | ***ex vivo*** | **digitized** |
| BA1_exvivo | BA1_3 | 1034.5 | 4772.5 | 772 | 0.7460 | 0.1620 |
| BA2_exvivo | BA2 | 2433.5 | 4307.5 | 2204 | 0.8985 | 0.5235 |
| BA3a_exvivo | BA1_3 | 1121.5 | 4772.5 | 865 | 0.7692 | 0.1804 |
| BA3b_exvivo | BA1_3 | 2018 | 4772.5 | 1961.5 | 0.9690 | 0.4100 |
| BA4a_exvivo | BA4 | 1803.5 | 6625 | 1660.5 | 0.9388 | 0.2475 |
| BA4p_exvivo | BA4 | 1349.5 | 6625 | 1207 | 0.8864 | 0.1805 |
| BA6_exvivo | BA6 | 6578 | 9617.5 | 4278.5 | 0.6444 | 0.4407 |
| BA44_exvivo | BA44 | 1606.5 | 2688 | 1279 | 0.8057 | 0.4832 |
| BA45_exvivo | BA45 | 1722.5 | 4062 | 1164.5 | 0.6690 | 0.2835 |
| V1_exvivo | BA17 | 4589.5 | 6027 | 3802 | 0.8286 | 0.6341 |
| V2_exvivo | BA18 | 5198 | 6430 | 2705.5 | 0.5220 | 0.4210 |
| | mean | 2677.7 | 5518.1 | 1990.9 | 0.7889 | 0.3606 |
| | std | 1806.0 | 1823.6 | 1158.9 | 0.1536 | 0.1608 |

**Application to HCP subjects**

Figure S1-S5 are illustrations of the digital atlases applied to an additional five HCP subjects to illustrate the cross-individual consistency of the atlases on external MR data. Figures show the pial surface of the left hemisphere of HCP subject 101915 (Figure S1), 102816 (Figure S2), 103515 (Figure S3), 106016 (Figure S4) and 101107 (Figure S5), overlaid with the digital atlases of Campbell (A), Smith (B), Brodmann (C), Flechsig (D), Von Economo (E) and Kleist (F).

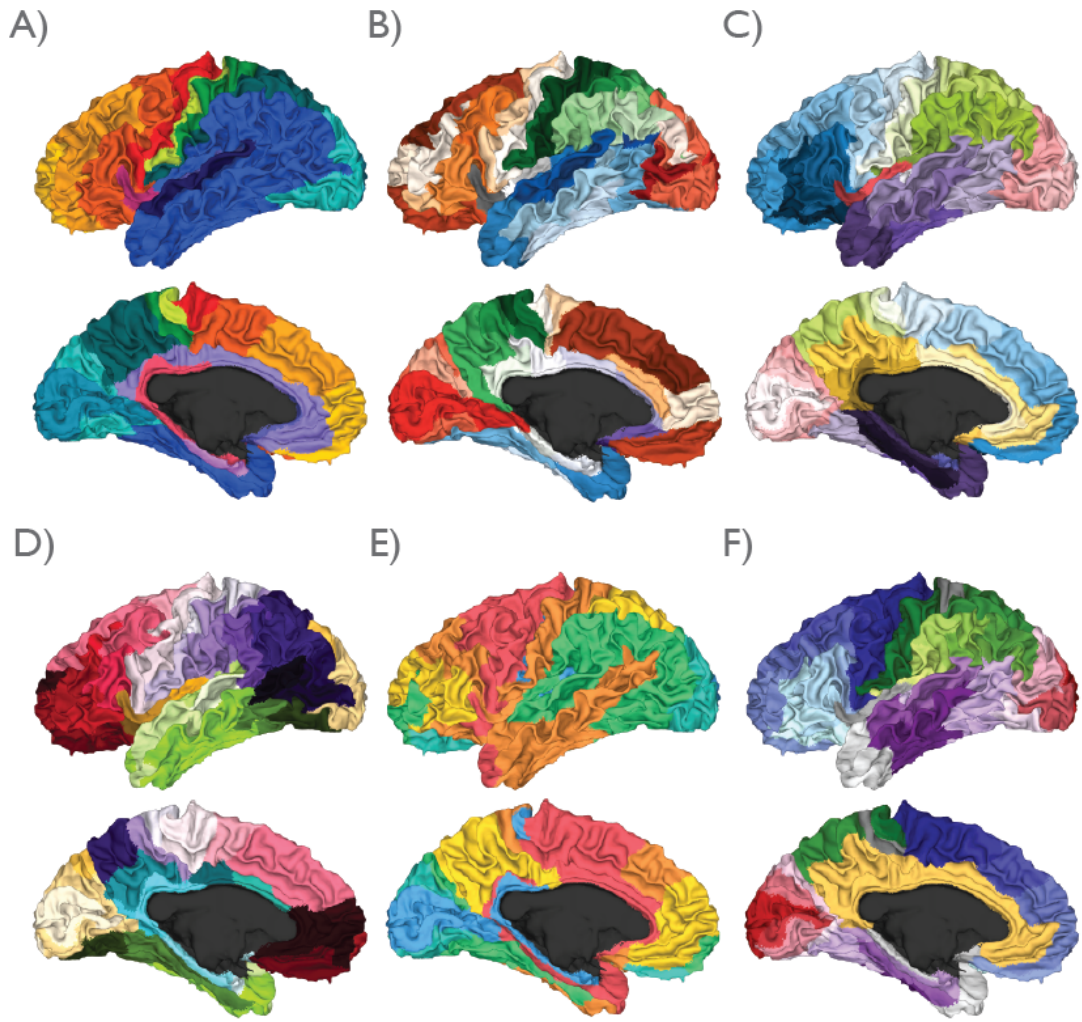


**Figure S1. Application of the digital atlases to HCP subject 101915.** All six digital atlases are visualized on the white matter surface of the left hemisphere of HCP subject 101915. Lateral and medial images of the digital atlases originally constructed by **A)** Campbell, **B)** Smith, **C)** Brodmann, **D)** Flechsig, **E)** Von Economo - cortical type and **F)** Kleist.

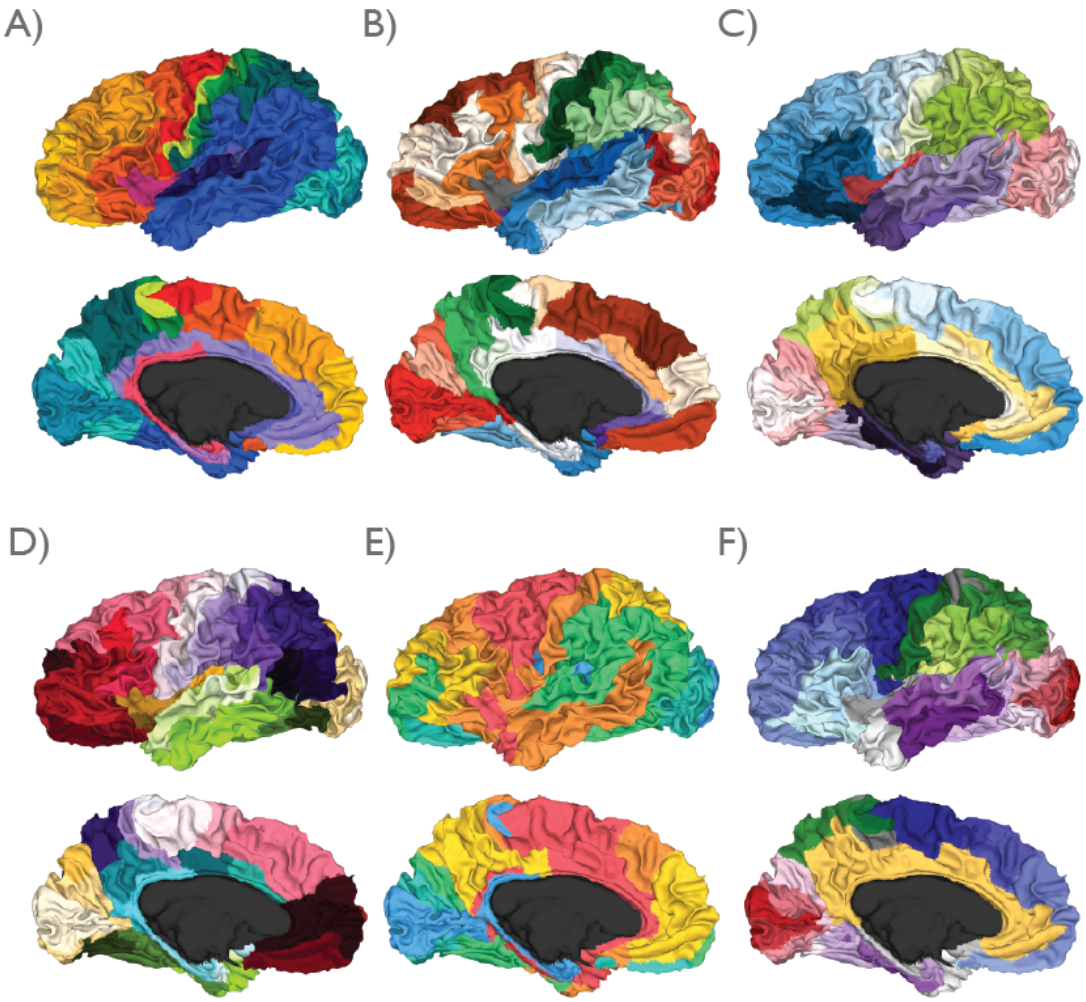


**Figure S2. Application of the digital atlases to HCP subject 102816.** All six digital atlases are visualized on the white matter surface of the left hemisphere of HCP subject 102816. Lateral and medial images of the digital atlases originally constructed by **A)** Campbell, **B)** Smith, **C)** Brodmann, **D)** Flechsig, **E)** Von Economo - cortical type and **F)** Kleist.

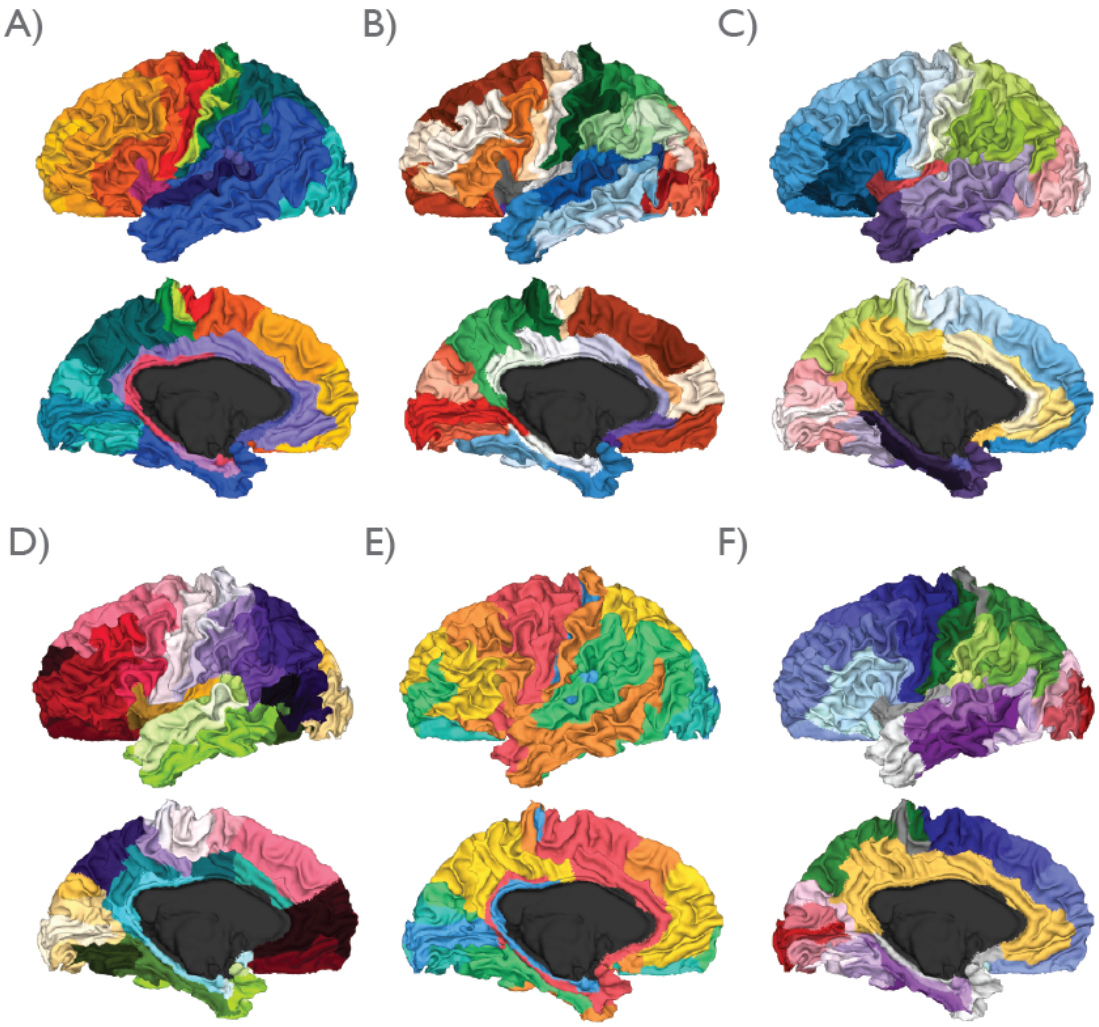


**Figure S3. Application of the digital atlases to HCP subject 103515.** All six digital atlases are visualized on the white matter surface of the white matter surface of the left hemisphere of HCP subject 103515. Lateral and medial images of the digital atlases originally constructed by **A)** Campbell, **B)** Smith, **C)** Brodmann, **D)** Flechsig, **E)** Von Economo - cortical type and **F)** Kleist.

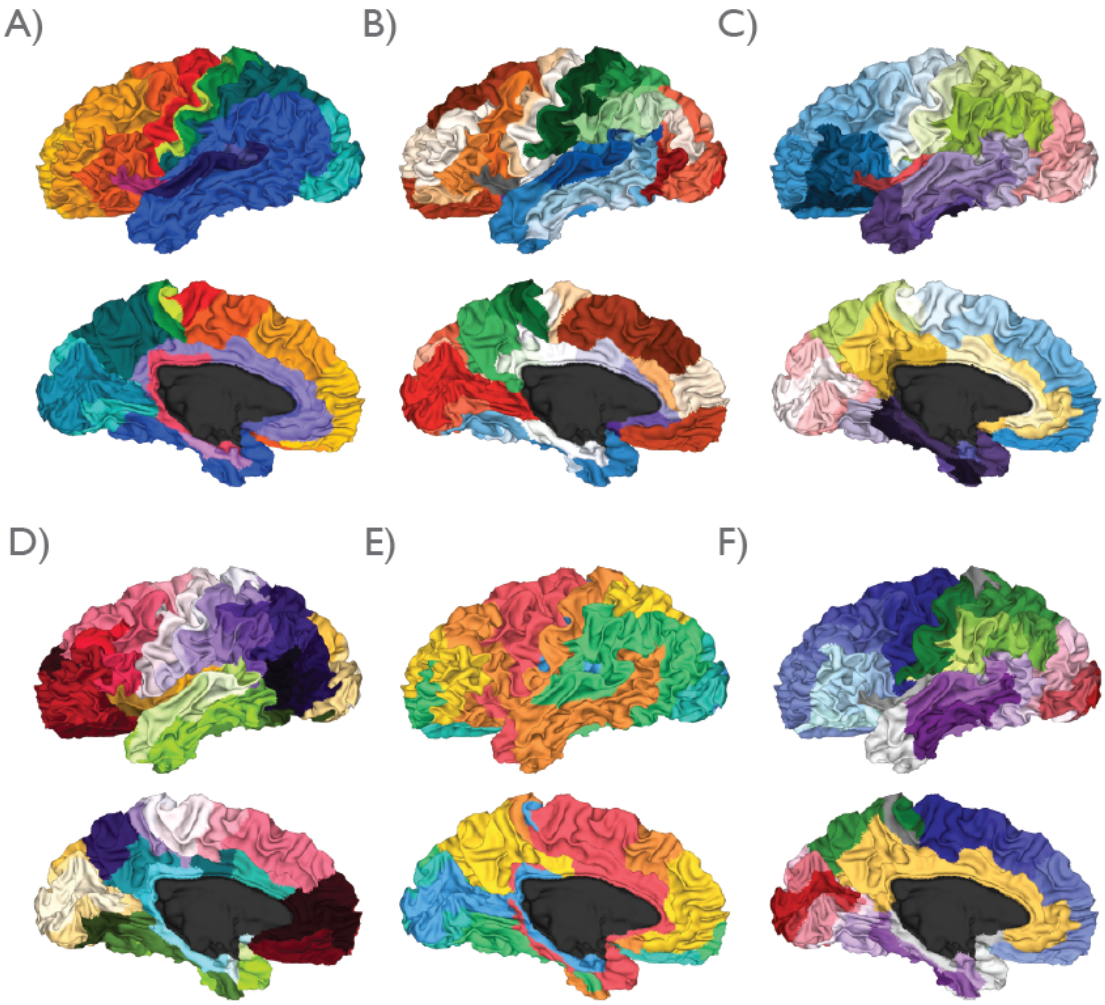


**Figure S4. Application of the digital atlases to HCP subject 106016.** All six digital atlases are visualized on the white matter surface of the left hemisphere of HCP subject 106016. Lateral and medial images of the digital atlases originally constructed by **A)** Campbell, **B)** Smith, **C)** Brodmann, **D)** Flechsig, **E)** Von Economo - cortical type and **F)** Kleist.

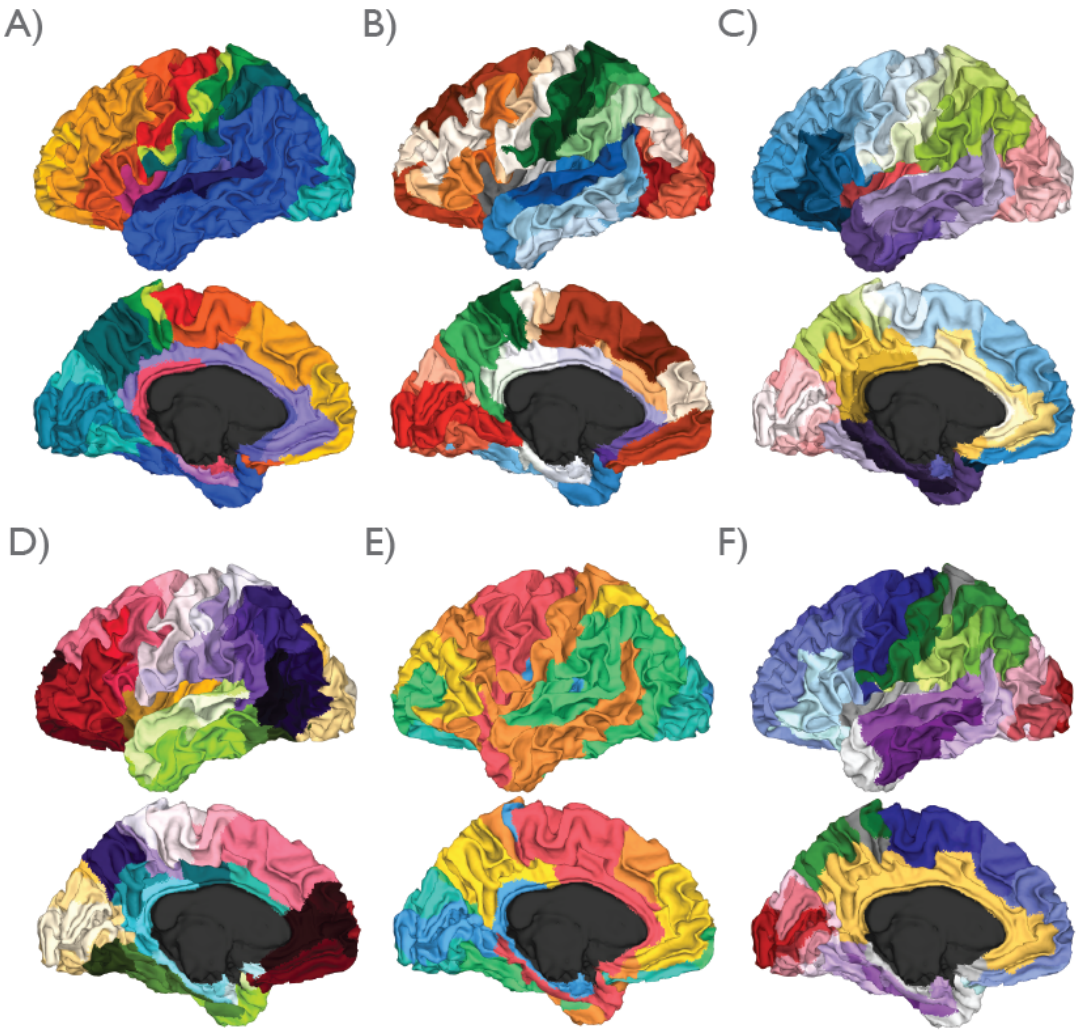


**Figure S5. Application of the digital atlases to subject 101107.** All six digital atlases are visualized on the white matter surface of the left hemisphere of subject 101107. Lateral and medial images of the digital atlases originally constructed by **A)** Campbell, **B)** Smith, **C)** Brodmann, **D)** Flechsig, **E)** Von Economo - cortical type and **F)** Kleist.

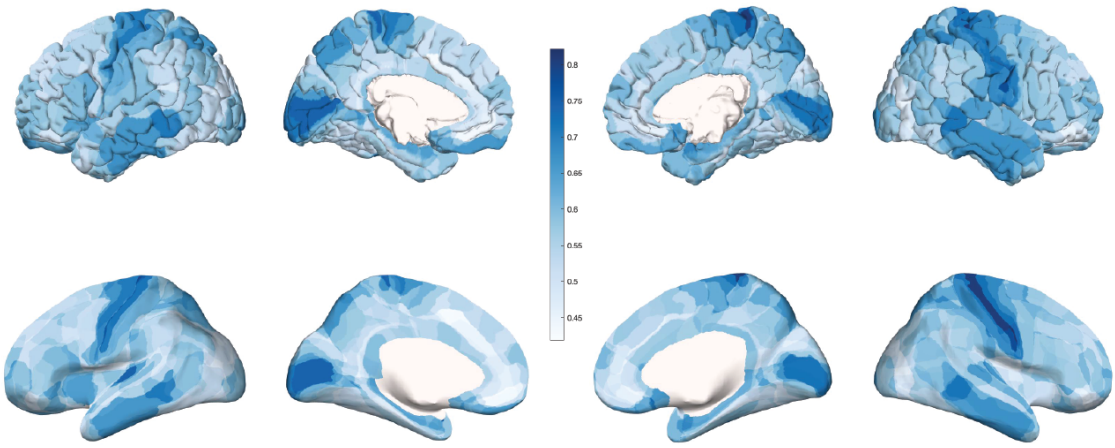


**Figure S6. Average vertex-wise region consistency across the set of six atlases**. Figure shows average region consistency maps of the left and right hemisphere, depicted on the *pial* surface (top) and *inflated* surface (bottom). Areas of high consistency are shown in dark blue (e.g. primary visual cortex) and low consistency in light blue (e.g. superior frontal cortex) consistency.

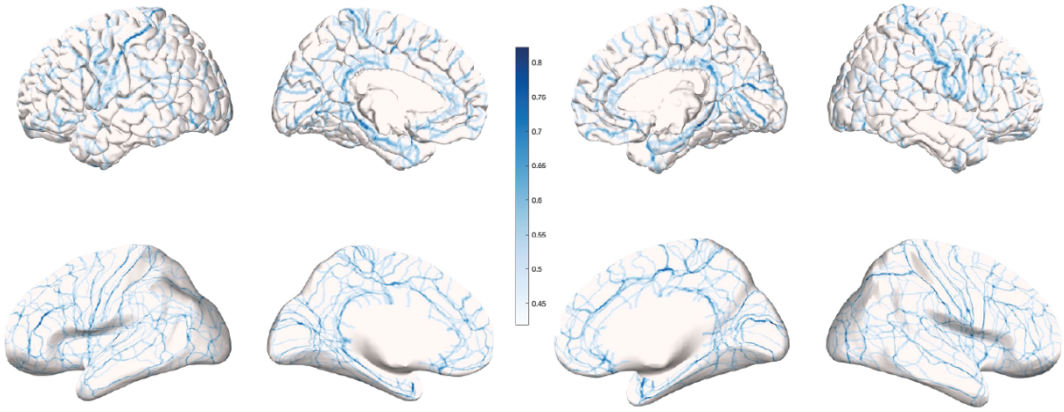


**Figure S7. Vertex-wise spatial consistency of region boundary placement across atlases**. Figure shows average boundary placement consistency maps of the left and right hemisphere, depicted on the *pial* surface (top) and *inflated* surface (bottom). In both hemispheres, highest consistency is observed at borders of primary cortical areas and between cortical parts with distinct cortical types, and more variable boundary placement in more higher order areas of the cortex.

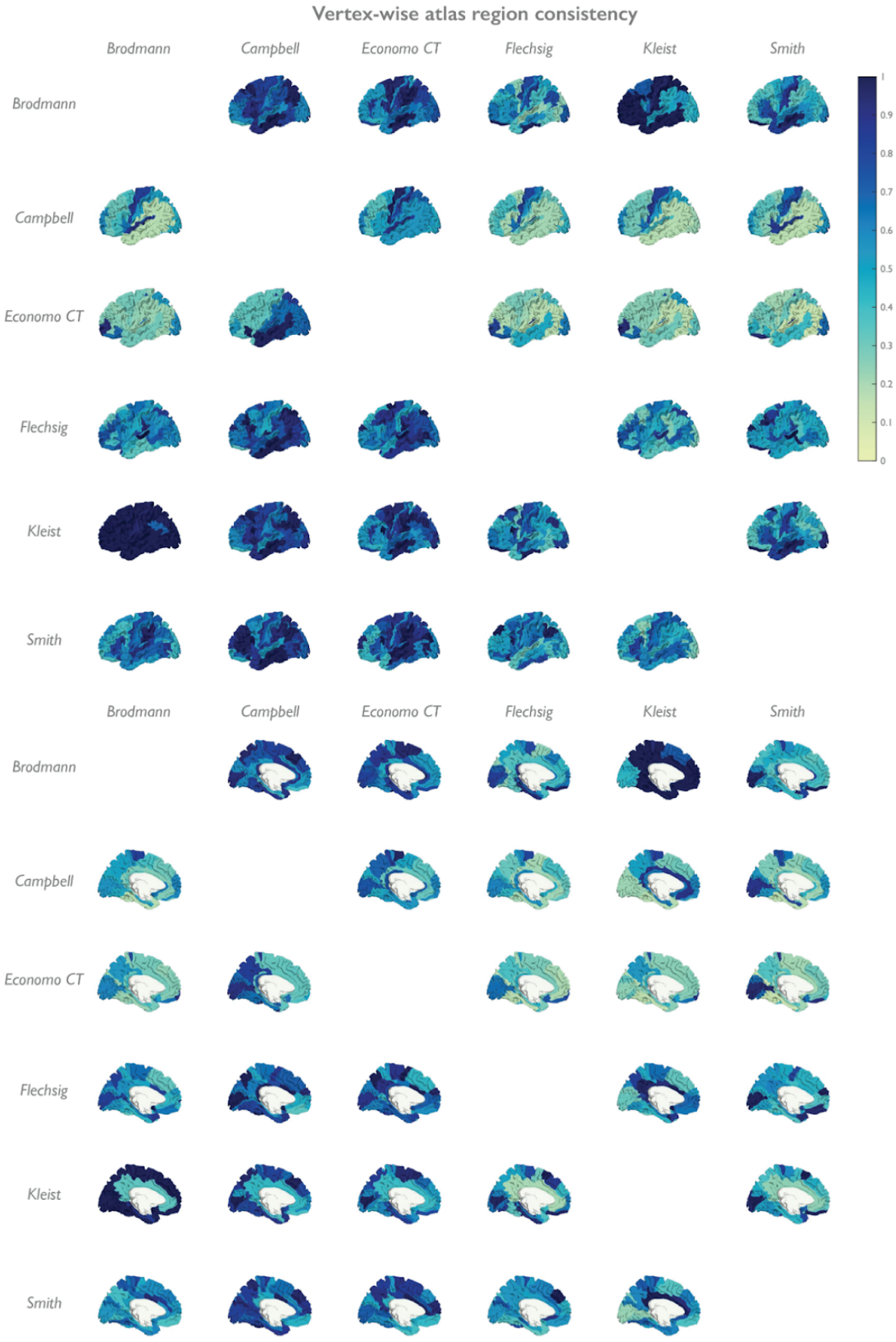


**Figure S8. Vertex-wise atlas-pair region consistency maps.** Each map in this figure represents the consistency of a given atlas' vertex region assignment with that of one of the other five atlases, shown for the lateral (top panel) and medial aspect (bottom panel) of the left hemisphere.

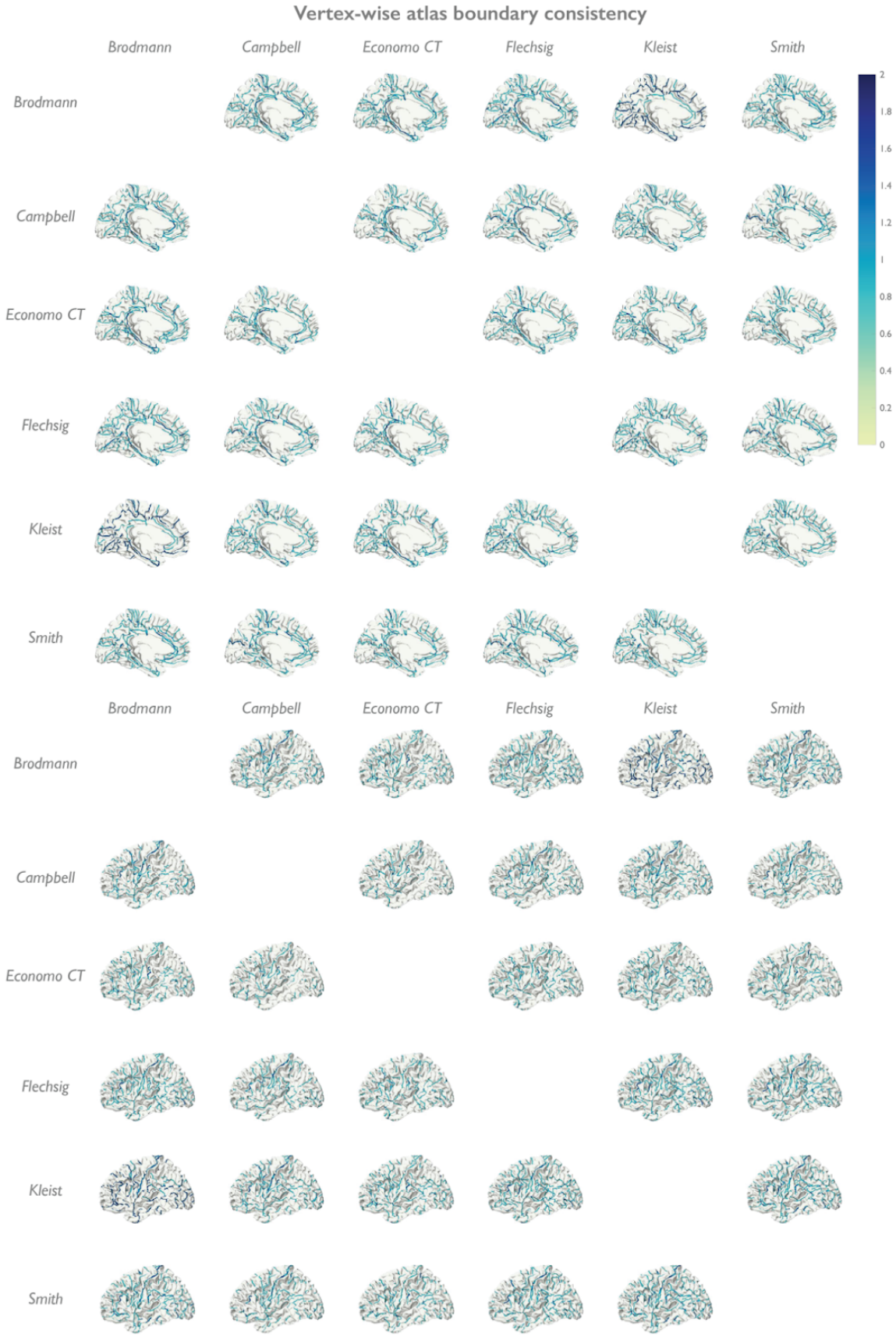


**Figure S9. Vertex-wise atlas-pair boundary consistency.** Each map in this figure represents the consistency of a given atlas' boundary with that of one of the other five atlases, for the left (top panel) and the right hemisphere (bottom panel).

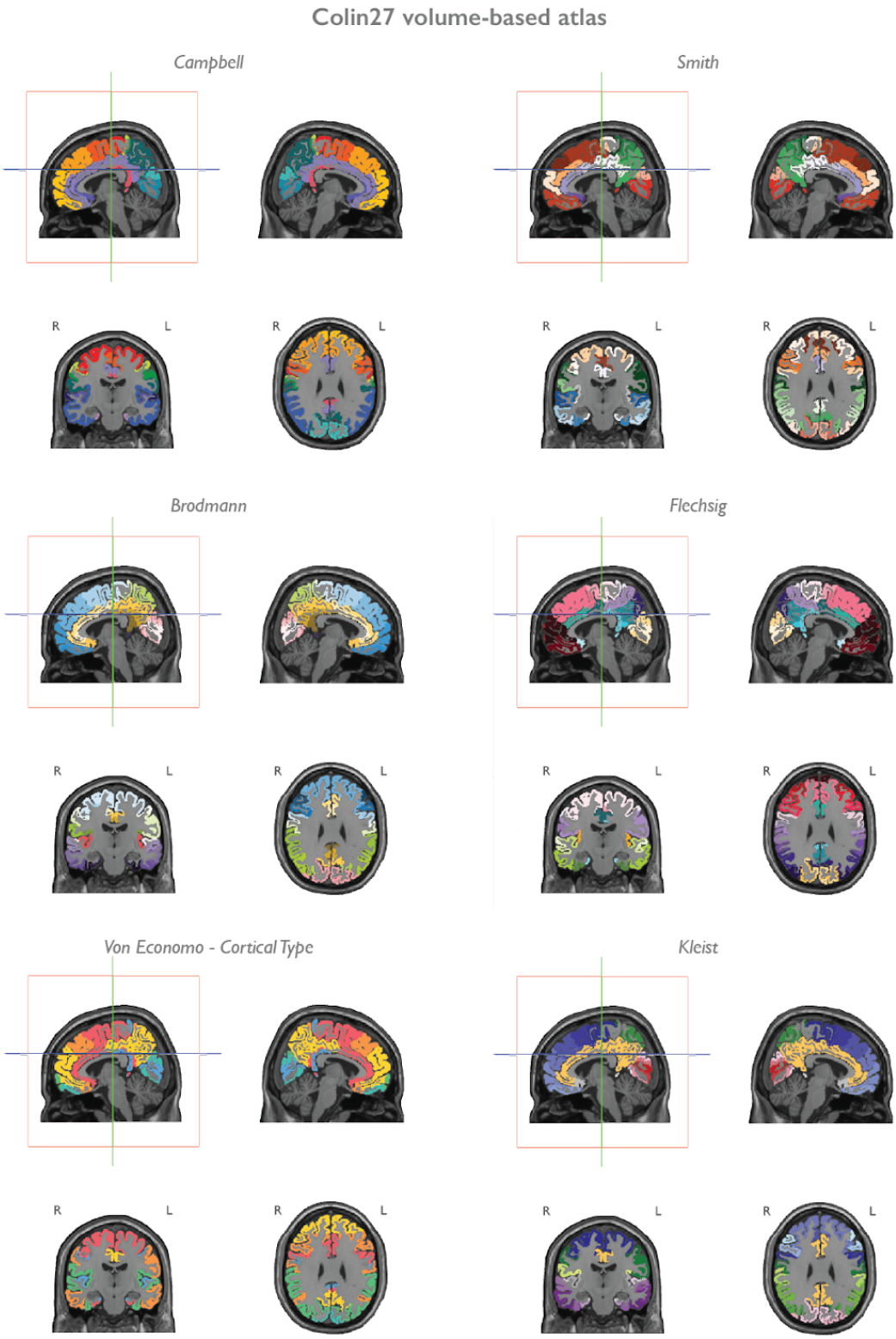


**Figure S10. Colin27 volume-based atlases.** Figure shows cross-sectional images of the transformed-to-volumetric space digitized atlases on the Colin27 template brain.

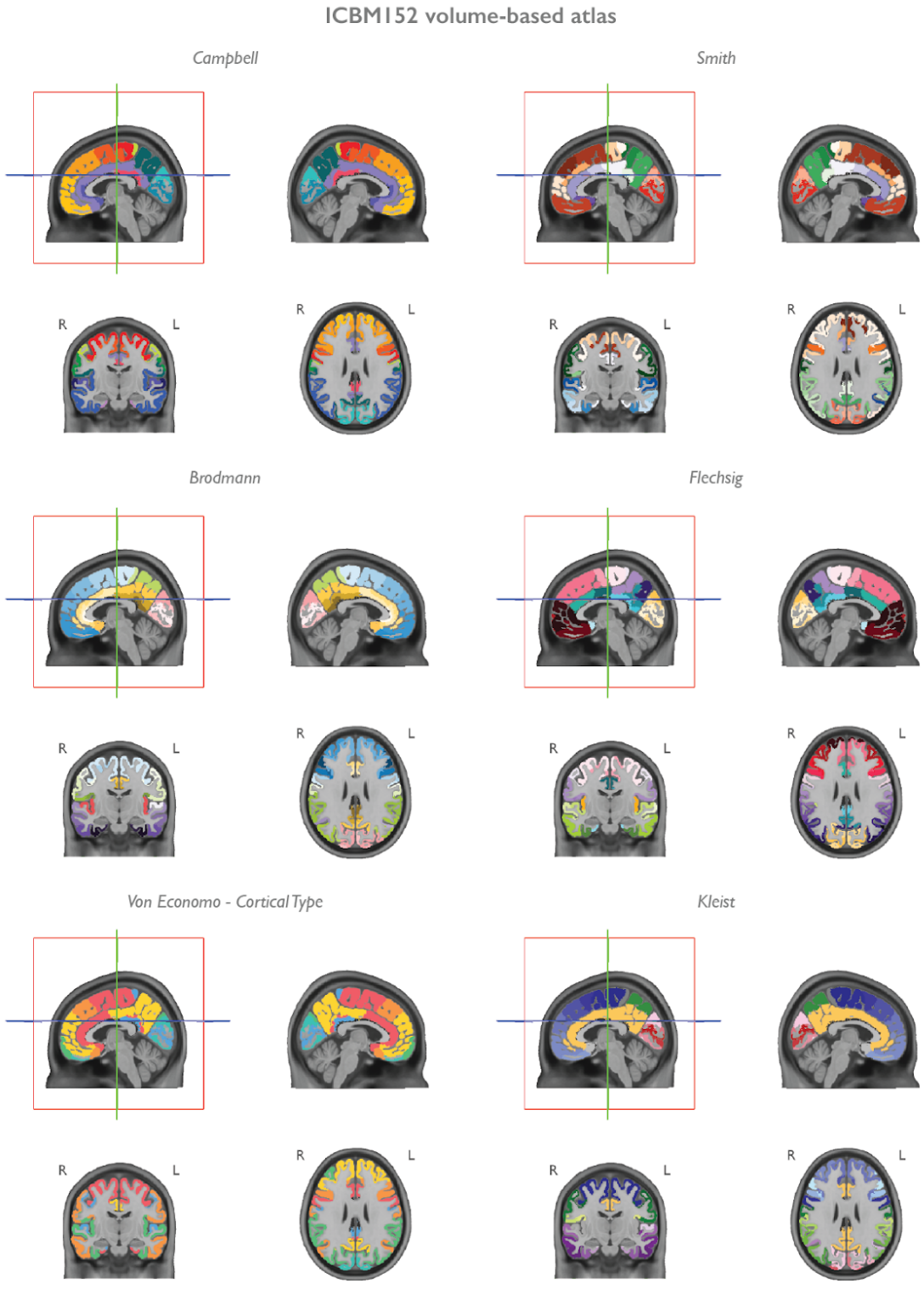


**Figure S11. ICBM152 volume-based atlases.** Figure shows cross-sectional images of the transformed-to-volumetric space digitized atlases on the ICBM152 average brain.

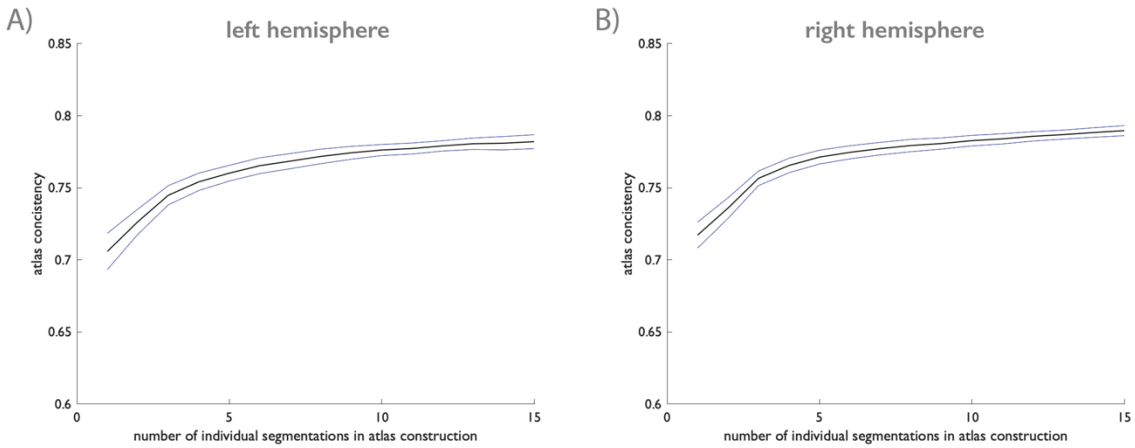


**Figure S12. Consistency of atlases built on 1 to 15 segmentations.** Consistency of automatic region label assignment with manually drawn labels computed in the set of 20 individual segmentations incorporated in the digitized Von Economo – Koskinas atlas (Scholtens et al., 2018). In a sliding window approach, *.gcs* atlases were constructed based on N=1 up to N=15 individual segmentations, then tested for vertex-wise label consistency with the manual segmentations of the remaining N=5. **A)** and **B)** depict the average effect (black line) of the number of individual segmentations incorporated in the atlas construction process on the region label consistency, together with the 95% confidence interval in blue for the left and right hemisphere respectively.

**References**

Brodmann, K. (1909). Vergleichende Lokalisationslehre der Grosshirnrinde in ihren Prinzipien dargestellt auf Grund des Zellenbaues, Barth.

Campbell, A. W. (1905). Histological studies on the localisation of cerebral function, University Press.

Flechsig, P. E. (1920). Anatomie des menschlichen Gehirns und Rückenmarks auf myelogenetischer Grundlage, G. Thieme.

Kleist K. (1934): Gehirnpathologie.

Smith, G. E. (1907). "A new topographical survey of the human cerebral cortex, being an account of the distribution of the anatomically distinct cortical areas and their relationship to the cerebral sulci." Journal of anatomy and physiology 41(Pt 4): 237.

Scholtens LH, de Reus MA, de Lange SC, Schmidt R, van den Heuvel MP. (2018): An MRI Von Economo - Koskinas atlas. Neuroimage 170:249-256.

von Economo, C. F. and G. N. Koskinas (1925). Die cytoarchitektonik der hirnrinde des erwachsenen menschen, J. Springer.